AGE DETERMINATION OF 15 OLD TO INTERMEDIATE-AGE SMALL MAGELLANIC CLOUD STAR CLUSTERS

M. C. PARISI[1], D. GEISLER[2], G. CARRARO[3], J. J. CLARIÁ[1], E. COSTA[4],
A. J. GROCHOLSKI[5], A. SARAJEDINI[6], R. LEITON[2], AND A. E. PIATTI[1]

[1] Observatorio Astronómico, Universidad Nacional de Córdoba, Laprida 854, Córdoba,
CP 5000, Argentina; celeste@oac.uncor.edu, claria@oac.uncor.edu, andres@oac.uncor.edu
[2] Departamento de Astronomía, Universidad de Concepción, Casilla 160-C, Concepción,
Chile; dgeisler@astro-udec.cl, roger.leiton@astro-udec.cl
[3] European Southern Observatory, Casilla 19001, Santiago de Chile, Chile; gcarraro@eso.org
[4] Universidad de Chile, Casilla 36-D, Santiago de Chile, Chile; costa@das.uchile.cl
[5] Department of Physics and Astronomy, Louisiana State University, 202 Nicholson Hall, Tower Drive, Baton Rouge,
LA 70803-4001, USA; grocholski@phys.lsu.edu
[6] Department of Astronomy, University of Florida, P.O. Box 112055, Gainesville, FL 32611, USA; ata@astro.ufl.edu

ABSTRACT

We present color–magnitude diagrams in the *V* and *I* bands for 15 star clusters in the Small Magellanic Cloud (SMC) based on data taken with the Very Large Telescope (VLT, Chile). We selected these clusters from our previous work, wherein we derived cluster radial velocities and metallicities from calcium II infrared triplet (CaT) spectra also taken with the VLT. We discovered that the ages of six of our clusters have been appreciably underestimated by previous studies, which used comparatively small telescopes, graphically illustrating the need for large apertures to obtain reliable ages of old and intermediate-age SMC star clusters. In particular, three of these clusters, L4, L6, and L110, turn out to be among the oldest SMC clusters known, with ages of 7.9 ± 1.1, 8.7 ± 1.2, and 7.6 ± 1.0 Gyr, respectively, helping to fill a possible "SMC cluster age gap." Using the current ages and metallicities from Parisi et al., we analyze the age distribution, age gradient, and age–metallicity relation (AMR) of a sample of SMC clusters measured homogeneously. There is a suggestion of bimodality in the age distribution but it does not show a constant slope for the first 4 Gyr, and we find no evidence for an age gradient. Due to the improved ages of our cluster sample, we find that our AMR is now better represented in the intermediate/old period than we had derived in Parisi et al., where we simply took ages available in the literature. Additionally, clusters younger than ∼4 Gyr now show better agreement with the bursting model of Pagel & Tautvaišienė, but we confirm that this model is not a good representation of the AMR during the intermediate/old period. A more complicated model is needed to explain the SMC chemical evolution in that period.

Key words: galaxies: star clusters: general – Magellanic Clouds

Online-only material: color figures, extended figure

1. INTRODUCTION

As it is widely known, the Small Magellanic Cloud (SMC) is the closest dwarf irregular galaxy to the Milky Way (MW). For this reason, it is the ideal local analog to this type of primeval distant galaxy. Due to its low metallicity, the SMC constitutes an excellent field of study to explore the role played by metallicity in these galaxies. Star clusters of the Magellanic Clouds (MCs), particularly those of the SMC, are important to trace their chemical evolution and star formation history. Because of the richness and variety of the SMC star clusters, they are also important testbeds for theoretical models of stellar evolution at intermediate age and moderately low metallicity (e.g., Ferraro et al. 1995). Besides, the SMC clusters have been used as empirical templates to interpret the unresolved spectra and colors of distant galaxies (e.g., Beasley et al. 2002).

In order to study the early star formation history of a galaxy, it is crucial to characterize well the oldest stellar populations. Globular clusters (GCs) are ideal objects as tracers of the oldest populations. In addition, although the GC system of a galaxy exhibits an age range, the oldest GCs clearly belong to the oldest stellar systems that were formed in the early universe and still survive. In those galaxies where the age of the oldest field populations can be determined and compared with the age of the Galactic GCs, it was found that, in general, the age difference between these two populations is not significant within the errors and that the oldest GCs in different galaxies in the Local Group are coeval. This indicates a common epoch of initial star formation in the MW and its companions in the Local Group. However, the SMC is the only Local Group galaxy with a significant cluster population that seems not to share this common epoch of early cluster formation. In fact, although this galaxy has a large number of young and intermediate-age clusters, it contains only one cluster, NGC 121, confirmed to be older than 10 Gyr and considered the only known SMC GC, in the sense that its age is comparable to those of the bulk of the Galactic GCs. This has given rise to a series of speculations and controversies regarding the chemical evolution of the SMC and that of its companion, the Large Magellanic Cloud (LMC). NGC 121, however, is clearly not as old as the oldest GCs of the LMC or of the MW (Glatt et al. 2008a). In fact, NGC 121 has an estimated age of only 10.5 Gyr (Glatt et al. 2008a) instead of 12–12.5 Gyr found for the oldest clusters of the LMC and MW (e.g., Dotter et al. 2010). Even though recent efforts have uncovered at least one other SMC cluster approaching the age of NGC 121 (HW 42, with an age of 9.3 Gyr; Piatti 2011a), it is now clear that the SMC lacks the very oldest GCs that are found in other massive Local Group galaxies. The reason for this is currently unknown.

The next oldest cluster in the SMC currently known after NGC 121 and HW 42, L1, has an age of only 7.5 Gyr, based on deep *Hubble Space Telescope* (*HST*) data (Glatt et al. 2008a). Interestingly, the LMC has a well-known large cluster age gap between 3 and 12 Gyr within which only one cluster exists. We also know, however, that the LMC contains 15 or 16 clusters older than 10 Gyr (see, e.g., Dutra et al. 1999). The SMC indeed also has a potential cluster age gap (as suggested by Glatt et al. 2008a), with only two clusters presently known between 7.5 and 13.7 Gyr, a gap covering almost half the age of the galaxy since the big bang.

At present, there is no clear explanation for the lack of clusters in the so-called age gap in the LMC. Likewise, no scenario has been proposed for why there are no truly ancient clusters in the SMC or for its possible cluster age gap, although the latter has not been well studied and the sample size is quite small. The fact that NGC 121 is the only known relatively old SMC cluster means that all conclusions related to the early evolution of this galaxy's cluster system are based only on this single object. It is evident, in this context, that the discovery of other old clusters in the SMC would have important implications related to its early formation and chemical evolution, even clusters inhabiting the possible age gap between NGC 121 and L1.

Our group began investigating MC clusters using the powerful technique of Ca II triplet spectroscopy (CaT) with FORS2 on the Very Large Telescope (VLT) several years ago. As shown by Cole et al. (2004), CaT is a very efficient and accurate metallicity indicator, with minimal age effects. Our first study (Grocholski et al. 2006) yielded excellent data for 28 LMC clusters. We found a very tight metallicity distribution for intermediate-age clusters, no metallicity gradient, and confirmed that the clusters rotate with the disk. We followed this up with an initial study of SMC clusters (Parisi et al. 2009, hereafter Paper I). We used FORS2 + VLT to obtain CaT spectra of more than 100 stars in 15 populous SMC clusters, spanning a wide range of ages and metallicities. We derived velocities to a few km s^{-1} per star and mean cluster metallicity (from >7 high probability members) to 0.05 dex. We examined the metallicity distribution, metallicity gradient, the age–metallicity relation (AMR), and kinematics for the cluster sample. We found a suggestion of bimodality in the metallicity distribution, no evidence for a gradient, and a hint of rotation in our cluster sample, but the kinematics are dominated by the velocity dispersion.

While the cluster metallicities constituted a reliable as well as homogeneous source of information, since they were determined by applying the same well-proven technique, based on excellent data, cluster ages unfortunately are on a heterogeneous and relatively poorly determined scale. This results from the fact that we took the ages available from the literature, which were derived by applying several different methods. These clusters were selected mainly from color–magnitude diagrams (CMDs) in the Washington system published by Piatti et al. (2005, 2007b, 2007c), which were based on data obtained with the Cerro Tololo Inter-American Observatory (CTIO) 0.9 m telescope. Unfortunately, such data are not optimal for deriving accurate ages for old and intermediate-age SMC clusters, given the small aperture and large pixel scale. The lack of accuracy and homogeneity in the cluster ages limits our confidence in the study of the chemical evolution of the SMC, despite the excellent metallicities in hand.

In order to improve that situation, we decided to redetermine the ages of the 15 SMC clusters studied in Paper I on a homogeneous scale. As explained in that paper, before obtaining the CaT spectroscopic observations, the VLT staff obtained images of the selected clusters in the *V* and *I* bands. These images, usually called *pre-images*, were necessary to build the instrumental CMDs that allowed us to select the cluster red giants that were observed spectroscopically and to perform the requisite astrometry for these targets in order to ensure good slit positioning. Pre-images are not generally used for purposes other than this and thus are usually taken with the minimum exposure times necessary, in this case to obtain reasonable photometry for the upper red giant branch (RGB) of each cluster. This unfortunately prohibits using them for something as demanding as determining accurate ages, which requires good data to well below the main sequence. However, we realized that for a minimum additional cost in overhead we could lengthen the pre-images from the usual few second exposures to several minutes. Given the 8 m aperture and generally good to excellent seeing available, this ensured that these data would go much deeper than any available and would yield excellent material from which to derive ages. Thus, we put these pre-images to very good astrophysical use! However, in Paper I we only used the literature ages, as time did not permit us to obtain the required photometry. Also, Paranal Observatory does not provide standard star images in order to determine the transformation of magnitudes and colors to the standard system. Thus, standardizing the pre-images was problematic and we waited until we could find an appropriate solution. We have subsequently solved this either by obtaining independent calibration photometry and/or obtaining the ages differentially, without the need for standardization. Hence, the time was ripe for investigating the cluster ages.

In this paper, we report on the ages we derive for our cluster sample from the pre-images and related results. In Section 2, we detail the procedure used to obtain the uncalibrated photometry. Section 3 describes our initial age determination procedure. Next, we present the CMDs of each cluster and investigate two existing age calibrations. Here, we find that several of our clusters are substantially older than indicated by previous studies and indeed turn out to be among the oldest star clusters known in the SMC. Section 5 describes the importance of such clusters for examining the early chemical and dynamical evolution of the SMC. In addition, we derive a new age calibration appropriate for old to intermediate-age SMC clusters, which yields ages for our oldest clusters that support their extreme age. In order to further strengthen these results, we also present isochrone ages based on calibrated photometry we derive for the three most interesting old cluster candidates. In Section 6 we discuss our results, while Section 7 summarizes our findings.

2. OBSERVATIONS AND REDUCTIONS

Paper I gives all of the relevant details about the cluster sample. Basic information is given in Table 1, wherein we list the different cluster designations followed by their right ascension and declination, and the metallicity and semimajor axis *a* reported in Paper I (see Section 6.2 for details about calculation of *a*). The metallicities of the 15 clusters presented in Paper I were derived from the equivalent widths of the CaT lines, measured on the spectra of a number of cluster member red giants.

As we will see in the next section, there exist age calibrations that permit one to derive the age of a cluster from the difference between the magnitude of the red clump (RC) and the main sequence turnoff (MSTO). Since this involves a difference in magnitudes, we do not need calibrated photometry

Table 1
Cluster Sample

Cluster	R.A. (J2000.0) (h m s)	Decl. (J2000.0) (° ′ ″)	[Fe/H] (dex)	a (°)
BS 121 = SMC OGLE 237	01 04 22	−72 50 52	−0.66 ± 0.07	1.496
HW 47	01 04 04	−74 37 09	−0.92 ± 0.04	3.502
HW 84	01 41 28	−71 09 58	−0.91 ± 0.05	5.513
HW 86	01 42 22	−74 10 24	−0.61 ± 0.06	7.345
L4 = K1, ESO 28-15	00 21 27	−73 44 55	−1.08 ± 0.04	3.265
L5 = ESO 28-16	00 22 40	−75 04 29	−1.25 ± 0.05	3.092
L6 = K4, ESO 28-17	00 23 04	−73 40 11	−1.24 ± 0.03	3.124
L7 = K5, ESO 28-18	00 24 43	−73 45 18	−0.76 ± 0.06	2.888
L17 = K13, ESO 29-1	00 35 42	−73 35 51	−0.84 ± 0.03	1.718
L19 = SMC OGLE 3	00 37 42	−73 54 30	−0.87 ± 0.03	1.564
L27 = K21, SMC OGLE 12	00 41 24	−72 53 27	−1.14 ± 0.06	1.392
L106 = ESO 29-44	01 30 38	−76 03 16	−0.88 ± 0.06	7.877
L108	01 31 32	−71 57 10	−1.05 ± 0.05	4.460
L110 = ESO 29-48	01 34 26	−72 52 28	−1.03 ± 0.05	5.323
L111 = NGC 643, ESO 29-50	01 35 00	−75 33 24	−0.82 ± 0.03	7.830

in order to derive cluster ages through this procedure. When we programmed the spectroscopic observations, we deliberately had in mind the need to re-derive cluster ages in a homogeneous way, so we requested that VLT staff extend the pre-image exposure times. We used exposure times of 200 s and 100 s in the I and V bands, respectively, in addition to the usual short exposures required to not saturate the brightest giants.

FORS2 has two 2k × 4k CCDs. Pixels were binned 2 × 2, providing a plate scale of 0″.25 pixel^{-1}. Target clusters were centered on the master CCD (upper), while the secondary CCD (lower) was used to observe field stars. The observations were performed with a typical seeing less than 1″. The pre-images were corrected for bias and flat-field following the usual procedure using IRAF,[7] while the point-spread-function (PSF) photometry was performed using the DAOPHOT/ALLSTAR packages, independent from IRAF (Stetson 1987).

Figure 1 shows, as an example, the typical behavior of color and magnitude errors (upper and lower panels, respectively) as a function of instrumental magnitude. For magnitudes less than 15, most stars have $\sigma_v < 0.03$ and $\sigma_{v-i} < 0.05$, for the bulk of cluster. For some clusters, for example, L17, L27, and L111, these errors are larger, probably due to the greater degree of crowding in the core regions.

3. MORPHOLOGICAL AGE INDEX

One way to derive cluster ages uses a morphological index that quantifies observational parameters in the CMD that are sensitive to age (Anthony-Twarog & Twarog 1985; Janes & Phelps 1994; Rosenberg et al. 1999). A differential method, which utilizes differences between well-observed parameters to derive age, is particularly powerful as it is insensitive to photometric problems, reddening, distance, etc. This technique allows the derivation of cluster ages, avoiding the well-known difficulties present in the isochrone fitting method (Vandenberg et al. 1990; Sarajedini & Demarque 1990; Salaris & Weiss 1997), but requires accurate calibration with fiducial clusters.

Phelps et al. (1994) and Janes & Phelps (1994, hereafter JP94), respectively, defined the δV parameter as the difference between the visual magnitude V of the MSTO (V_{TO}) and that
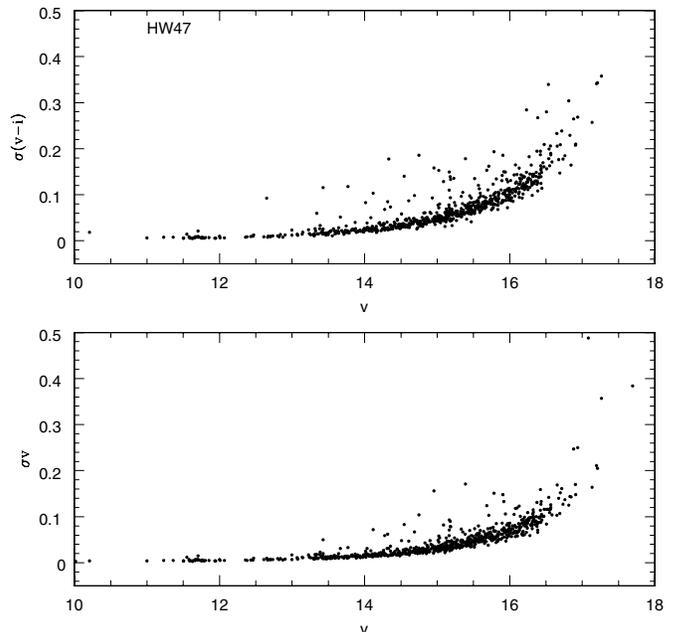
Figure 1. Photometric errors in v and $v - i$ as a function of instrumental v magnitude for cluster HW 47.

of the RC (V_C) (see Figure 1 of Phelps et al. 1994). It is well known that the MSTO luminosity depends on the cluster age but that the RC luminosity is almost age independent (Cannon 1970); therefore, δV turns out to be a good and reliable age indicator. JP94 showed that there is a good correlation between the parameter δV and the cluster age, in the sense that the younger the cluster, the smaller the δV value. Due to the heterogeneity of the calibration material, JP94 emphasize the fact that their calibration can only be used to make a ranking of clusters in terms of age and is not robust for absolute age determinations. For this reason, Carraro & Chiosi (1994, hereafter CC94) and, more recently, Salaris et al. (2004, hereafter S04) recalibrated the relation between age, metallicity, and δV, based on homogeneous Galactic cluster samples.

Both calibrations include a metallicity dependence, but, because this dependence is small, in cases where there is no information regarding the cluster metallicity, the metallicity-dependent term can be neglected (CC94). Despite having

information about the metallicity of our clusters, we decided to neglect the metallicity term because those clusters used for the derivation of all available $t - \delta V -$[Fe/H] calibrations (for example, S04 and CC94) are galactic clusters that cover a metallicity range very different from the one covered by our cluster sample, which is considerably more metal-poor. Since we are trying to derive ages of SMC clusters that have a very different chemical evolution from those of our Galaxy, the metallicity issue is relevant. It is for this reason plus the fact that metallicity terms are small that we will not consider the metallicity effect on age. We note that the systematic effects from uncertainty on the basis of the CC94 (and S04) relations and the neglect of any metallicity compensation means that the uncertainties in the derived ages are likely larger in many cases than the errors stemming from determining δV. A revised δV age calibration explicitly taking into account the chemical composition of both SMC and LMC star clusters is needed.

One of the most reliable methods to derive cluster ages is isochrone fitting. However, the CMDs necessary to apply such a method must be based on calibrated photometry. As noted above, our PSF photometry was performed on VLT pre-images and we did not have the calibration images necessary to transform magnitudes and colors to the standard system. We then decided to use the δV method as our primary age determinant since it does not rely on calibrated photometry.

4. CLUSTER AGES

4.1. Color–Magnitude Diagrams and Age Determination

Before starting the analysis of the observed cluster CMDs, it is necessary to minimize their contamination by field stars. Such contamination clearly constitutes an important factor that limits precision in the determination of all cluster parameters, particularly $V_{\rm TO}$. To decrease the field star contamination in the CMDs, we followed the procedure described by Piatti et al. (2005), that is, to build CMDs including stars located in different concentric circular areas centered on the cluster center. Then we qualitatively analyzed the ratio of field to cluster stars within each ring by studying their variation as a function of radius.

Figures 2(a)–(o) show the instrumental CMDs built from the DAOPHOT output, corresponding to circular regions centered on each cluster. For each cluster, we built four different CMDs, which include stars belonging to four radial ranges of 100 pixel width each. The first diagram (top left panels) includes all of the stars located within a circle of 100 pixel radius. The following two diagrams (top right and bottom left panels) include all of the stars between 100 and 200 pixels and from 200 to 300 pixels from the cluster center, respectively. The fourth diagram (bottom right panels) includes all of the stars with distances from the cluster center greater than 300 pixels.

It can be clearly seen that the first diagram (inner interval) is, as expected, the least contaminated by field stars. The second annular CMD is still dominated by cluster stars, although the field contamination has increased considerably and is beginning to dominate the cluster stars in the third annular CMD. Therefore, to identify the CMD features of interest (V_C and $V_{\rm TO}$), we decided to use the CMDs constructed with stars belonging to the two innermost regions, that is, those located within 200 pixels from the center. Figures 3(a)–(d) show the CMDs of our cluster sample constructed using only the aforementioned annuli. These CMDs were used to determine V_C and $V_{\rm TO}$. As can be seen in Figures 3(a)–(d), all clusters exhibit reasonably well-defined RCs and MSTOs, except clusters BS 121, L17, and

L27, in which the dispersion near the MSTO is comparatively higher. In these cases, of course, the determination of the MSTO is clearly more uncertain. To quantify contamination by field stars in the CMD of Figures 3(a)–(d), we calculated the "contamination index": since we know the field star surface density surrounding the cluster, i.e., in the $r > 300$ pixel region, we calculated the number of field stars within an $r = 200$ pixel circle. The ratio between this number and the real number of (cluster + field) stars inside the said circle is a measure of the field star contamination. This parameter is listed in the last column of Table 2. It is seen that contamination is very high for BS 121, strong for HW 47, L17, L19, and L27, relatively small for HW 84, HW 86, L5, L6, and L7, and very low for the remaining clusters. Clearly, ages derived for clusters in the two most contaminated categories will have larger errors.

Because the determination of δV includes some degree of subjectivity, three members of our team determined this parameter independently. Since these three independent determinations generally showed good agreement (total spread of 0.1–0.5 in δV), we then adopted the value of δV corresponding to the average of such determinations. We estimated that a typical error in the determination of both V_C and $V_{\rm TO}$ is 0.2 mag, which implies an uncertainty of $\sim$0.3 mag for δV. However, the range in such factors as contamination among our sample means that this adopted typical error is likely too small in some cases and too large in others. Then we estimated ages using both the S04 and CC94 calibrations. From here on, we will refer to the ages derived from the calibrations of S04 and CC94 t_S and t_C, respectively.

In Table 2 we list the cluster designations, δV, t_S, and t_C, and their respective errors. The errors were calculated using error propagation on the corresponding equation. We also include in the table the age values reported in the literature, t_L, as well as the reference to the corresponding work where t_L was determined. Finally, we list the "contamination index" described above.

As can be seen from Table 2, t_S is systematically larger than t_C for all clusters. This tendency becomes considerably larger for older clusters. We compared ages derived for both the CC94 and S04 prescriptions to those found by Glatt et al. (2008b) for seven old to intermediate-age SMC clusters using deep *HST* data and state-of-the-art isochrones. These ages are among the best constrained of any SMC clusters. This comparison is presented in Figure 4. It is clear that CC94 ages are in much better agreement with those of Glatt et al. (2008b) for all clusters. Based on these arguments, for the subsequent analysis, we use ages estimated from the CC94 calibration. However, it is important to note that, although CC94 ages are in better agreement with Glatt's ages than those of S04, there is a significant offset even between ages from Glatt et al. (2008b) and those derived using the CC94 calibration, with the CC94 ages being larger by about a Gyr on average, independent of age. More precisely, the difference between both values goes from 0.29 to 2.02 Gyr with a mean value of 1.22 (standard deviation of 0.61). This difference may arise from the fact that, as already mentioned, the SMC and Galactic clusters used by CC94 as calibrators have very different chemical compositions. Again, a new age calibration for the chemical composition of the MCs is sorely needed.

4.2. Comparison with Previous Age Determinations

To compare our age determinations with those from other authors, we show t_L in Figure 5 as a function of the age
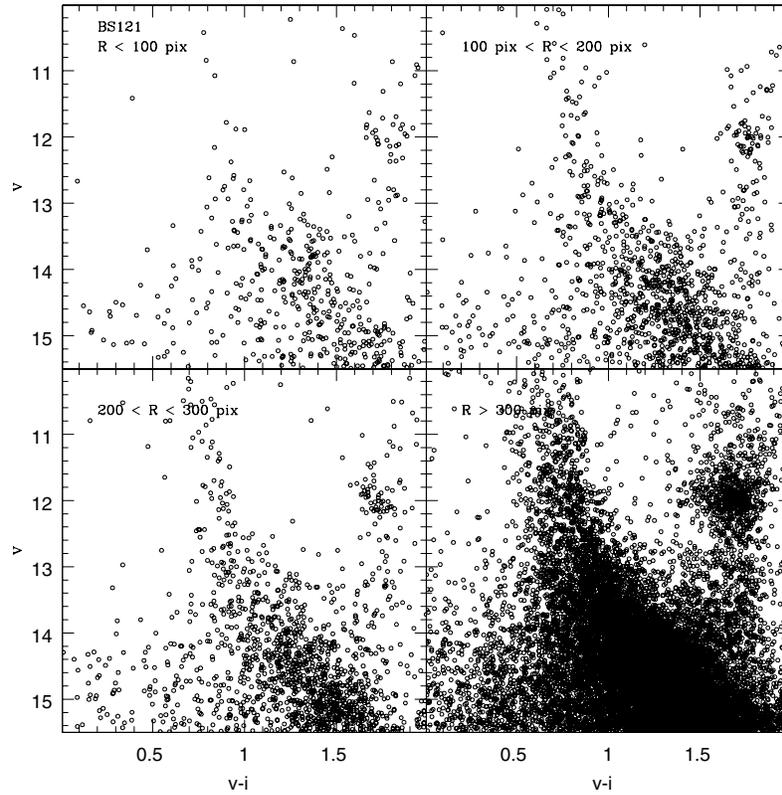
Figure 2. (a) Instrumental color–magnitude diagram for cluster BS 121, built from the DAOPHOT output. Each panel corresponds to a radial extraction. The selected radial intervals for each extraction are shown in the plot. (b) Same as (a) but for cluster HW 47. (c) Same as (a) but for cluster HW 84. (d) Same as (a) but for cluster HW 86. (e) Same as (a) but for cluster L4. (f) Same as (a) but for cluster L5. (g) Same as (a) but for cluster L6. (h) Same as (a) but for cluster L7. (i) Same as (a) but for cluster L17. (j) Same as (a) but for cluster L19. (k) Same as (a) but for cluster L27. (l) Same as (a) but for cluster L106. (m) Same as (a) but for cluster L108. (n) Same as (a) but for cluster L110. (o) Same as (a) but for cluster L111.

(An extended version of this figure is available in the online journal.)

Table 2
Cluster Ages

Cluster	δV (mag)	t_S (Gyr)	t_C (Gyr)	t_L (Gyr)	t_L Reference	Contamination Index
BS 121	1.89 ± 0.30	3.5 ± 0.5	2.8 ± 0.5	2.30	1	0.86
HW 47	2.07 ± 0.30	4.3 ± 0.7	3.3 ± 0.5	2.80	1	0.59
HW 84	1.39 ± 0.30	2.1 ± 0.3	1.6 ± 0.2	2.40	1	0.35
HW 86	1.23 ± 0.30	1.7 ± 0.2	1.4 ± 0.2	1.60	1	0.40
L4	2.91 ± 0.30	12.3 ± 2.1	7.9 ± 1.1	3.10	1	0.21
L5	2.17 ± 0.30	4.9 ± 0.8	3.7 ± 0.5	4.10	1	0.30
L6	3.00 ± 0.30	13.8 ± 2.4	8.7 ± 1.2	3.30	1	0.32
L7	1.45 ± 0.30	2.2 ± 0.3	1.6 ± 0.2	2.00	1	0.29
L17	2.34 ± 0.30	5.9 ± 0.9	4.4 ± 0.6	1.26	2	0.54
L19	2.43 ± 0.30	6.6 ± 1.1	4.8 ± 0.7	2.10	1	0.50
L27	2.39 ± 0.30	6.3 ± 1.0	4.6 ± 0.6	2.10	1	0.52
L106	1.58 ± 0.30	2.5 ± 0.4	2.0 ± 0.3	0.89	3	0.13
L108	1.93 ± 0.30	3.7 ± 0.6	2.9 ± 0.4	0.89	3	0.17
L110	2.87 ± 0.30	11.6 ± 1.9	7.6 ± 1.0	6.40	4	0.09
L111	1.57 ± 0.30	2.5 ± 0.4	2.0 ± 0.3	1.00	3	0.06

References. (1) Piatti et al. 2005; (2) Rafelski & Zaritsky 2005; (3) Piatti et al. 2007c; (4) Piatti et al. 2007b.

values found in the current study (t_C). The solid line represents the 1:1 relation between both quantities. From this diagram, we classified the clusters in three different groups: the ages of the nine clusters identified with circles are in reasonably good agreement with those previously derived by other authors, while the remaining clusters of the sample exhibit age values reported in the literature that are lower than the ones derived in this work, which is more remarkable for squares than for triangles.

Triangles and squares represent clusters where t_L is moderately and considerably smaller than t_C, respectively. To make this discrimination, we adopted the following criteria: we first calculated the difference between t_L and t_C and then we compared that difference with the mean error of t_C ($\bar{\sigma}_{tc}$), which is 0.54 Gyr. If the difference $t_L - t_C$ is lower than $3\bar{\sigma}_{tc}$, we consider that the value of t_L is in agreement with the value of t_C (circles). If the difference is larger than $3\bar{\sigma}_{tc}$ but smaller than $6\bar{\sigma}_{tc}$, we consider
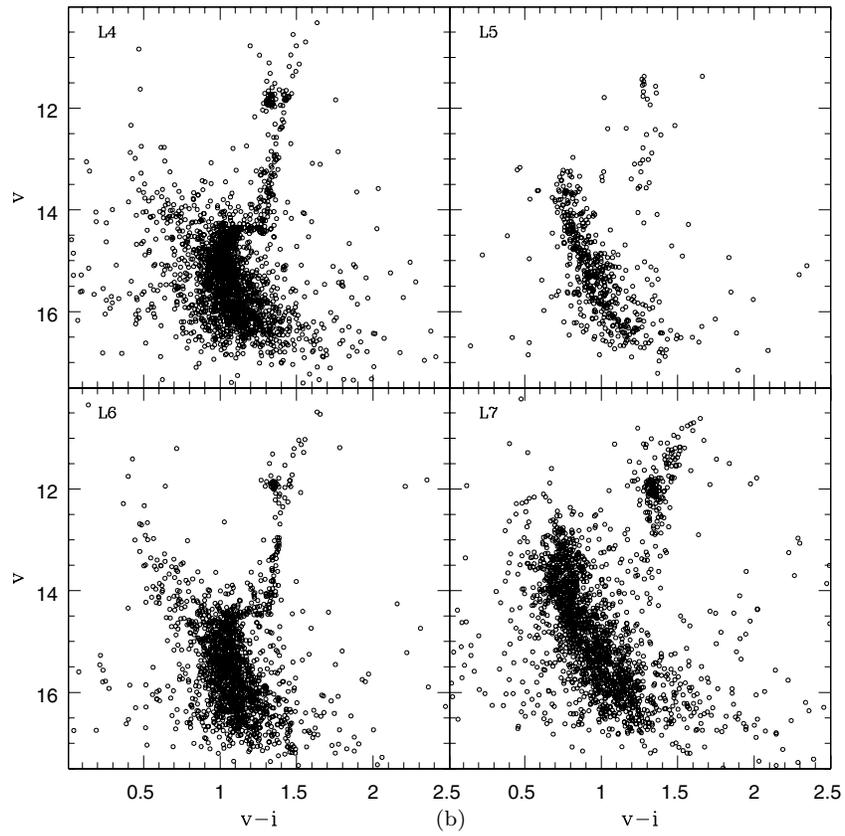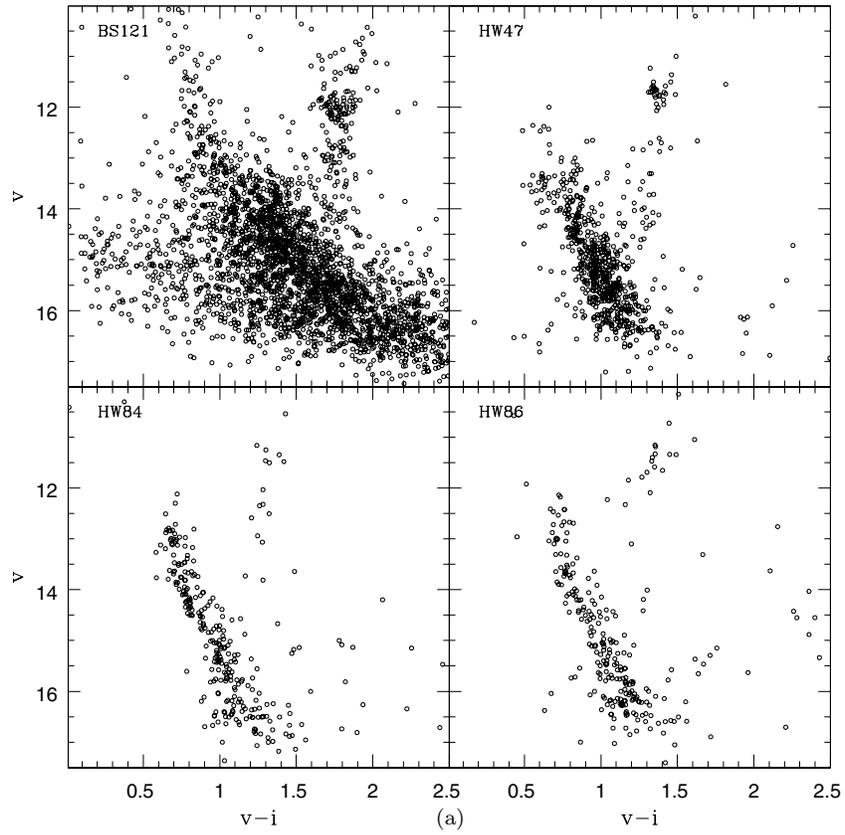
Figure 3. (a) Color–magnitude diagram built with stars belonging to the two first rings (0 pixels < r < 200 pixels) for clusters BS 121, HW 47, HW 84, and HW 86. (b) Same as (a) but for clusters L4, L5, L6, and L7. (c) Same as (a) but for clusters L17, L19, L27, and L106. (d) Same as (a) but for clusters L108, L110, and L111.
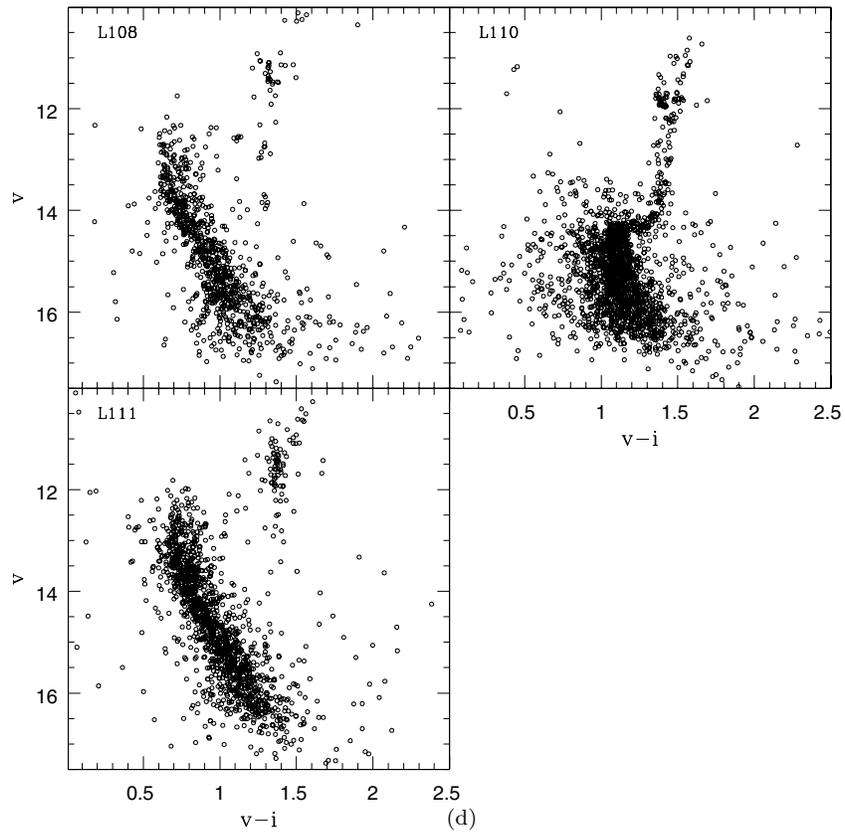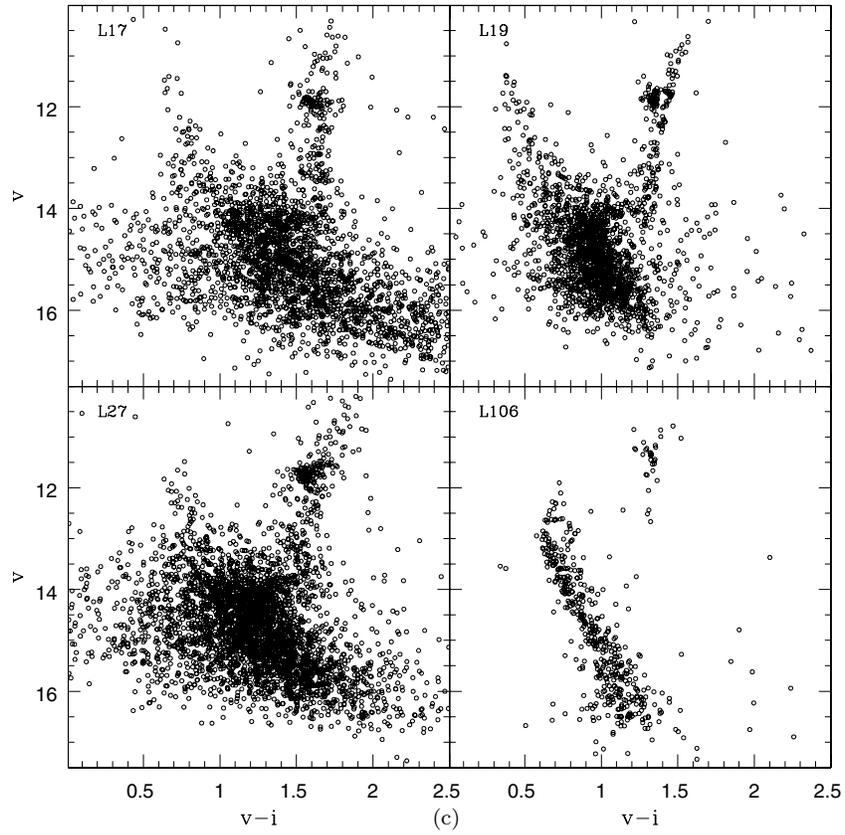
Figure 3. (Continued)
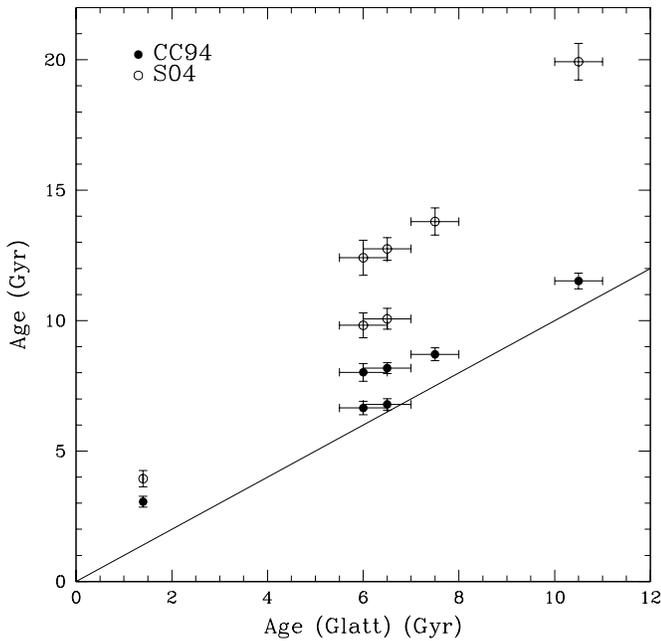
Figure 4. Comparison of ages derived with CC94 and S04 calibrations for clusters from Glatt et al. (2008b). The solid line represents the 1:1 relation.

Figure 5. Comparison of the ages reported in the literature (t_L) and the ages derived in this work (t_C) for the clusters of our sample. Clusters presenting good agreement between both age values have been plotted with circles. Triangles and squares represent clusters with a moderate and a considerable disagreement between t_L and t_C, respectively (see the text for more details).

that the disagreement between t_L and t_C is moderate (triangles). Finally, if the difference $t_L - t_C$ is larger than $6\bar{\sigma}_{t_C}$, then both age determinations exhibit a considerable disagreement (squares). The mean differences between t_L and t_C and their corresponding standard deviations are 0.7 ± 0.4, 2.7 ± 0.5, and 5.1 ± 0.4 Gyr for consistent clusters, moderately inconsistent clusters, and highly inconsistent clusters, respectively. Note that all of the inconsistent clusters have ages derived here that are larger than those found in the literature. The two highly inconsistent clusters are L4 and L6, which clearly stand out from the other clusters as being much older than previous indications. Much more will be said about these intriguing clusters in the next section.

The values of t_L for clusters L4, L6, L27, and L19 were derived by Piatti et al. (2005) following a procedure similar to ours. Using the $(T_1, C - T_1)$ CMDs, they derived the parameter δT_1 (difference between the T_1 magnitude of the RC and the MSTO). This parameter allows one to determine the age of a cluster from the calibration of Geisler et al. (1997). Note that this calibration included a wide range of metallicity, covering that of the majority of our cluster sample here, so metallicity effects should be minimal. The most likely explanation for the differences found between t_L and t_C is that the $(T_1, C - T_1)$ CMDs of these clusters are not deep enough to reach the corresponding MSTO with sufficient photometric accuracy to define this feature well. This fact may have led Piatti et al. (2005) to underestimate δT_1, which, in turn, implies a significant underestimation of the t_L value. The photometric observations used in the current study were obtained with an 8 m telescope, while those of Piatti et al. (2005) used a 0.9 m telescope. At a given magnitude, the photometric errors of the 8 m telescope observations are roughly a factor of three less than those from the 0.9 m telescope. As such, not only do the 8 m data extend to deeper magnitudes, but they do so with greater precision. Given the much smaller telescope, the difficulties in reaching the fainter portions of the cluster CMDs are more problematic, especially for older clusters in which the MSTO occurs at fainter magnitudes. It is then to be expected that the difference between

t_L and t_C is more noticeable for the older clusters of our sample (L4 and L6), as shown in Figure 5. In addition, both the seeing as well as the telescope scale represent important factors that tend to decrease the quality of Piatti et al.'s data compared to ours. In fact, the photometric data used by Piatti et al. (2005) were obtained with a seeing of 1″5 and a scale of 0″4 pixel^{-1}, while our pre-images were obtained with a seeing typically smaller than 1″ and a scale of 0″25 pixel^{-1}.

Regarding cluster L17, the value of t_L was estimated by Rafelski & Zaritsky (2005) from the comparison of the cluster integrated colors ($U - B$, $B - V$, and $V - I$) with models of simple stellar populations. As these authors point out, however, this work lacks accuracy in the calculated ages, mainly because the integrated colors have low precision and the models used do not predict consistent colors for a given age. As Rafelski & Zaritsky (2005) emphasize, their cluster ages should only be taken as a guide for future investigations. As for the cluster L108, its t_L value was derived by Piatti et al. (2007c) by fitting theoretical isochrones to the Washington system CMD. Recently, Piatti et al. (2011) derived ages for L108 of 1.10 ± 0.25 and 1.60 ± 0.30 Gyr, by fitting theoretical isochrones and by using the δT_1 parameter, respectively. According to the above described criteria, the L108 isochrone age is still moderately inconsistent but its morphological age is consistent with the value derived in this work. Again, the most likely reason for the discrepancy is that the Piatti et al. data are from a much smaller telescope (in this case a 1.5 m) with inferior seeing and scale.

5. OLD SMC CLUSTERS

As mentioned in the previous section, two of our clusters (L4 and L6) appear much older than indicated by previous studies. Indeed, our data strongly suggest that they are indeed very old SMC clusters, helping to fill the possible age gap between L1 and NGC 121.

To corroborate the very old nature of L4 and L6, we decided to perform independent age determinations. In addition, although the age of L110 derived here is consistent with the value reported in the literature (within the errors), our age of 7.6 Gyr based on the CC94 calibration officially makes L110 slightly older than L1, providing another "age-gap" cluster and a third very interesting object to be more thoroughly investigated, which we do here.

It is worth mentioning that Piatti (2012) recently found that the SMC cluster ESO 51-SC09 appears to be quite old, with an age (7.0 Gyr) comparable to that of L1. He calculated the parameter δV and used the JP94 calibration to derive the cluster age. He then transformed δV into δT_1 according to Equation (3) of Geisler et al. (1997) and calculated ESO 51-SC09's age from Equation (4) of the same work. Finally, he fitted theoretical isochrones of Marigo et al. (2008). He derived age values of 8.3 ± 1.6, 6.5 ± 1.0, and 6.3 ± 1.0 Gyr from δV, δT_1, and isochrone procedures, respectively. Piatti (2012) averaged these three values, obtaining an age of 7.0 ± 1.3 Gyr. However, as we have already mentioned, the JP94 calibration suffers from serious problems that render it less reliable for deriving accurate ages, and in particular, it overestimates ages, especially for older clusters. Using the δV value reported by Piatti (2012, 2.5 ± 0.15 Gyr) and the CC94 calibration, we derive an age of 5.2 ± 0.4 Gyr for ESO 51-SC09, which is 3 Gyr less than the value reported by Piatti (2012) using the JP94 calibration. This value turns out to be in better agreement with those derived from δT_1 and isochrone fitting. If we calculate the average of the three values from δV, δT_1, and isochrone fitting, using the CC94 instead of the JP94 calibration, ESO 51-SC09 has an age of 6.0 ± 1.4 Gyr. Though the average age derived in the present work is in agreement with the average age derived by Piatti (2012), within the errors, ESO 51-SC09 is now younger than L1, which supports the view that the JP94 calibration needs to be used with caution.

NGC 361 is another cluster that Piatti (2012) suggested may be older than L1. He reports for this cluster an age of 8.1 ± 1.2 Gyr derived by Mighell et al. (1998), but this value corresponds to the age NGC 361 would have if we assumed that L1 is 9 Gyr. This is obviously not the case because L1 now has a very well determined age of 7.5 Gyr (Glatt et al. 2008b). Mighell et al. (1998) actually derived an age of 6.8 ± 0.5 Gyr for NGC 361 and then added 1.3 ± 1.1 Gyr to this value in order to place its age on the scale of Olszewski et al. (1996). This allows us to conclude that the only currently known cluster candidates to lie in the possible "SMC age gap" between L1 and NGC 121 are L4, L6, L110, and HW 42.

Based on samples of cataloged and well-studied SMC clusters, Piatti (2011a) performed a statistical study of clusters older than 2.5 Gyr. He found that only about seven old or relatively old clusters have yet to be found. We note, however, that a considerable number of clusters (used by Piatti 2011a) whose ages were determined from the MSTO were observed with small telescopes and relatively poor seeing conditions and pixel scale. Therefore, it is likely that the photometry of some clusters studied by these authors is not deep enough to delineate the MSTO clearly. In consequence, some of these clusters could have ages that are underestimated, as shown clearly in Figure 5, and which is the case for both L4 and L6.

5.1. The SMC δ Calibration

In order to obtain an independent age determination for our new candidate old SMC clusters L4, L6, and L110 based on
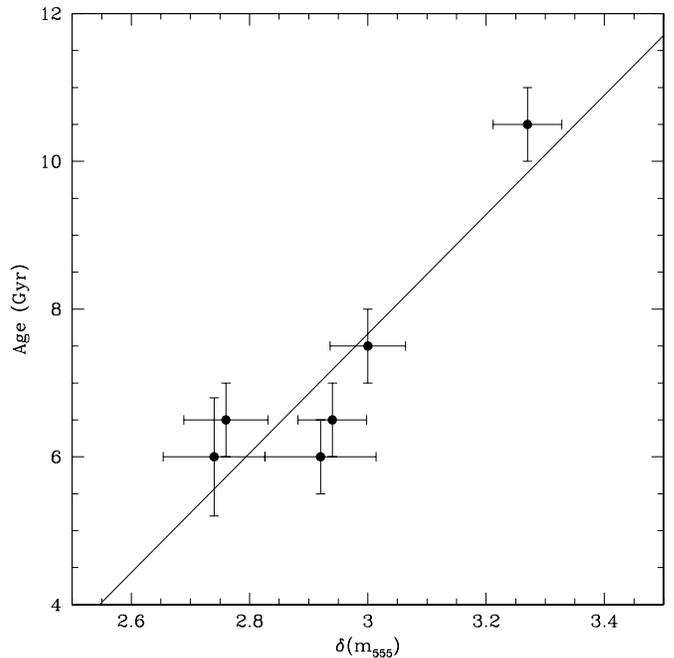
Figure 6. SMC δ calibration built with data taken from Glatt et al. (2008a, 2008b).

the best observed SMC clusters, we derived a new calibration (the "SMC δ calibration"), using the SMC clusters studied by Glatt et al. (2008a, 2008b). These authors observed the clusters Lindsay 1, Kron 3, NGC 339, NGC 416, Lindsay 38, NGC 419, and NGC 121 with *HST*. From a photometric analysis of their m_{555} versus $m_{555} - m_{814}$ CMDs, they reported the m_{555} magnitude of the MSTO and of the RC (see Table 2 of Glatt et al. 2008b). The difference between these values should be identical to δV. They also derived cluster ages using Padova (Girardi 2008; Girardi et al. 2000), Teramo (Pietrinferni et al. 2004), and Dartmouth isochrones (Dotter et al. 2007). We adopted their ages given by the Dartmouth isochrones because, as Glatt et al. (2008a, 2008b) note, this set of isochrones is the best approximation to the CMDs, except for NGC 419, in which Padova isochrones appear to be the best representation of its CMD. The Dartmouth age for NGC 121 is 10.5 ± 0.5 Gyr (Glatt et al. 2008a), while the Dartmouth ages for the other six observed clusters are given in Table 6 of Glatt et al. (2008b). The age of NGC 419 is rather uncertain because its CMD presents more than one MSTO. Hence, we decided not to include this cluster in the SMC δ calibration.

We present in Figure 6 the behavior of age as a function of δm_{555} using the Glatt et al. values. The best linear fit (solid line) is

$$\text{Age} = 8.1(\pm 1.9) \times \delta(m_{555}) - 16.6 \ (\pm 5.7), \qquad (1)$$

where age is given in Gyr. The fit has an rms of 0.83 Gyr. This "SMC δ calibration" is valid only for clusters older than ~ 6 Gyr with similar metallicities ([FeH] ~ -1) and can be applied to any V-band-like photometric system because it only involves a magnitude difference.

We then applied this calibration to our three old clusters, which indeed have metallicities similar to the Glatt sample (Parisi et al. 2009). We found ages for L110, L4, and L6 of 6.6, 6.9, and 7.7 Gyr, respectively. These values are in very good agreement with those found using the CC94 calibration (albeit showing the same offset found in Figure 4) but are more than

4 Gyr younger than the age calculated from the S04 calibration. This reaffirms our earlier suggestion that the S04 calibration overestimates age, which prompted us to choose the CC94 calibration. The error in age due to the error in δV is 2.42 Gyr. We added in quadrature this value and the rms dispersion of the linear fit which renders an age error of 2.5 Gyr. Note that, according to this procedure, all three clusters are about the same age as L1 at 7.5 Gyr, with L6 slightly older, and L4 and L110 a bit older than the next oldest clusters in the Glatt sample at 6.5 Gyr.

5.2. Fitting Isochrones

For another independent age determination for L4, L6, and L110, we also fit isochrones to the observed CMDs. As previously mentioned, our FORS2 photometry is uncalibrated because we do not have images of standard stars taken during the same night as the pre-images. We emphasize, however, that the three clusters were observed with FORS2 during the same night of 2005 August 8, in a time interval shorter than 1 hr. The night, according to VLT logs, was declared clear. For these reasons, the three clusters have been observed under the same, good sky conditions and at virtually the same airmass.

To tie the FORS2 images to the standard system, we obtained independent images of these three clusters, as well as images of standard stars, to perform the corresponding calibration of our PSF photometry using local standard stars (LSSs). From now on, for the sake of clarity, we will call CPIs the cluster pre-images and CCIs (cluster calibration images) the images obtained to calibrate the PSF photometry of the CPIs.

CCIs were obtained at the CTIO, using the Yale 1.0 m telescope, operated by the SMARTS consortium[8] during an observation run in 2010 December 8–10. The telescope works only in imaging mode with the Y4KCAM. This camera is equipped with an STA 4064 × 4064 CCD[9] with 15 μm pixels, yielding a scale of 0.''289 pixel^{-1} and a field of view of $20' \times 20'$ at the Cassegrain focus of the CTIO 1 m telescope. The CCD was operated without binning, at a nominal gain of 1.44 e^- ADU^{-1}, implying a readout noise of 7 e^- per quadrant (this detector is read by means of four different amplifiers).

The clusters were observed with exposures of 10, 60, and 600 s in both the V and I filters. To tie photometry to the standard system we observed the Landolt (1992) fields SA98 and T Phe three times during the night, spanning an airmass range from 1.03 to 2.10. SA98 is a particularly useful field since it contains more than 50 standard stars with a wide range in color.

After basic pre-processing, instrumental magnitudes were extracted following the PSF method (Stetson 1987). Aperture corrections were then determined for large aperture photometry of a suitable number (typically 10–20) of bright, isolated stars in the field. These corrections were found to vary from 0.190 in V to 0.200 in I. The PSF photometry was then aperture-corrected, filter by filter. Finally, calibrated magnitudes were obtained using the calibration solution inferred from the Landolt standards.

Once the PSF photometry of the CCIs was transformed into the standard system, we used it to calibrate the CPIs to the standard system. We proceeded as follows. (1) First, we selected as LSSs 97 stars from the CCI standard system photometry. (2) Second, we identified the LSSs in our CPI PSF photometry. (3) Next, we used the standard magnitudes and colors (V and

$V - I$) of the LSSs (obtained from the CCIs) and the instrumental magnitudes and colors (v and $v - i$) of the LSSs (obtained from the CPIs) to find the transformation coefficients to the standard system. (4) Finally, we applied the obtained transformation equations to all stars of the CPIs.

To select LSSs, we carefully chose bright stars that are as isolated as possible, avoiding stars located near the cluster centers that fell within our color range of interest (from the upper RGB to MSTO). LSSs have V magnitudes from $\sim$17.5 to $\sim$21 and colors $V - I$ from $\sim$-0.5 to $\sim$1.2.

We used the IRAF FITPARAM task to derive the transformation coefficients. Because we used LSSs, we fixed the airmass coefficients at zero. The equations and coefficients are

$$v = (-2.413 \pm 0.011) + V + (-0.037 \pm 0.012) \times (V - I) \quad (2)$$

$$i = (-2.137 \pm 0.016) + I + (0.023 \pm 0.019) \times (V - I), \quad (3)$$

where capital and lowercase letters represent standard and instrumental magnitudes, respectively. The rms are 0.036 and 0.096 for v and i fits, respectively. The standard magnitudes and colors of our observed stars were calculated by inverting Equations (2) and (3). The resulting CMDs for L4, L6, and L110 are presented in Figures 7(a)–(c), respectively.

To derive ages from isochrone fits, we followed the prescriptions given by Glatt et al. (2008b). Using the m_{555} versus $m_{555} - m_{814}$ CMDs, they fit three different models of isochrones: Padova, Teramo, and Dartmouth. We also fit, when possible, these three sets of isochrones to our own CMDs. Isochrone fits depend of course on many parameters, in particular cluster metallicity, reddening, and distance modulus (DM). We adopted cluster metallicities from Paper I, which were very accurately determined. Therefore, we have only two free parameters to adjust, reddening and DM. Although the SMC DM is assumed to be 18.88 (Storm et al. 2004), small adjustments to this parameter could be made in order to take into account the depth of the SMC in the line of sight (LOS).

According to Crowl et al. (2001), the LOS depth of the SMC ranges between 6 and 12 kpc. Consequently, it would seem reasonable to adopt 9 kpc as the mean value of the LOS depth. If we adopt 60 kpc for the mean SMC heliocentric distance and consider that star clusters can be located in front or behind the SMC, then their apparent DMs may present differences as large as 0.2 mag.

We fit Teramo and Dartmouth isochrones (upper and lower panels of Figures 8 and 9, respectively) to the CMD of L4 and L110, and Teramo and Padova isochrones (upper and lower panels of Figure 10, respectively) to the CMD of L6. We adopted a chemical composition $Z = 0.002$ ([Fe/H] $= -1.02$; Bertelli et al. 1994) for L4 and L110, and $Z = 0.001$ ([Fe/H] $= -1.33$; Bertelli et al. 1994) for L6, which are the closest to the observed values of these clusters.

In all cases, we adopted a set of isochrones and superimposed them on the CMDs, once they were shifted by the corresponding $E(V - I)$ color excess and by the apparent DM. Then we adopted, as the cluster age, the one corresponding to the isochrone that best reproduced the cluster fiducial ridgeline. The fitting parameters are shown in the corresponding plot (Figures 8 and 10).

We faced the following issue when we fitted isochrones to L4 and L6. The CMD of L4 is shifted to the blue by 0.035 mag (in $V - I$) with respect to the CMD of L6, as judged by their RCs and RGBs. These two clusters have virtually the same

---
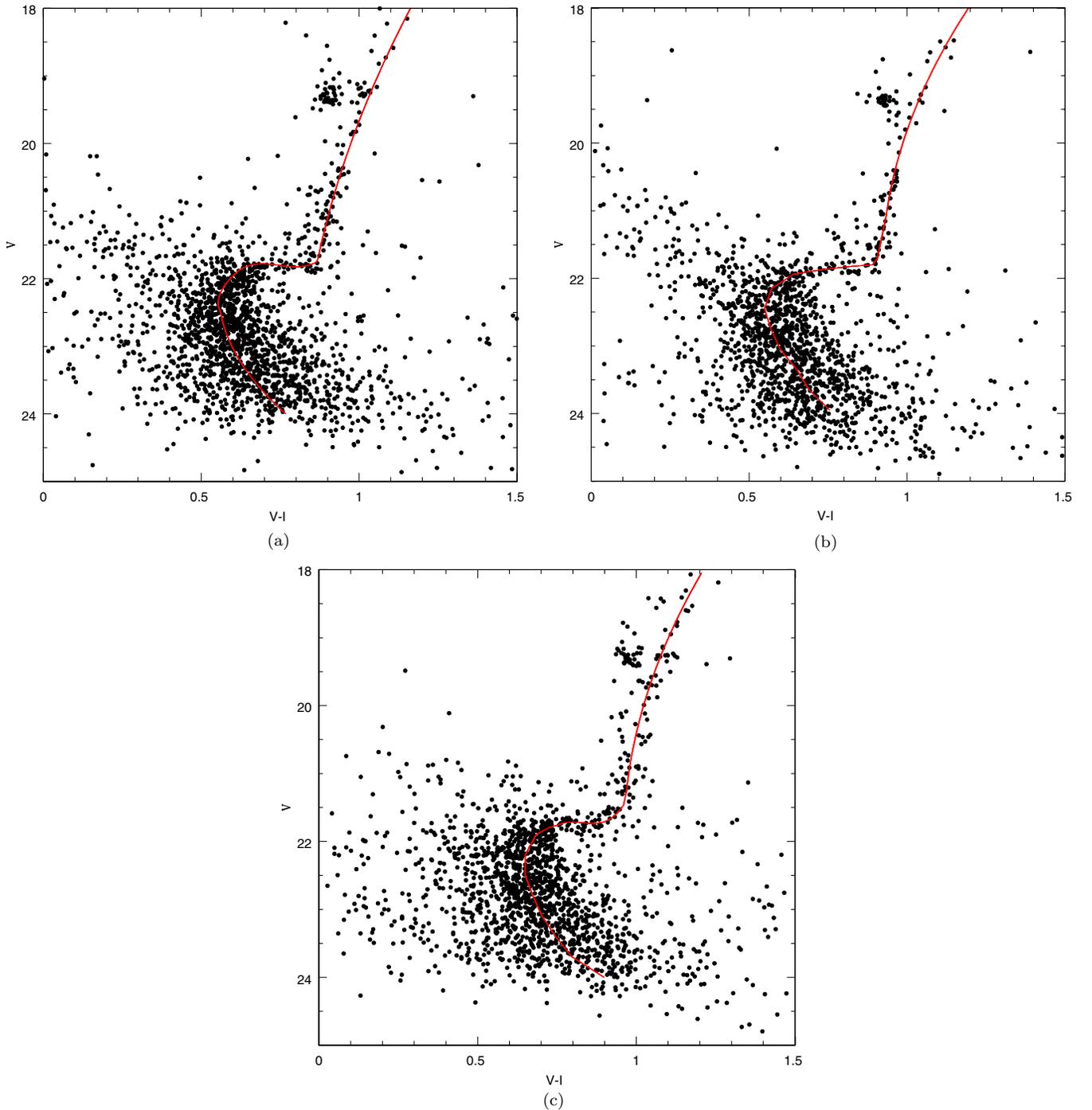
Figure 7. (a) Calibrated CMD of L4 built with stars with a distance from the cluster center smaller than 200 pixels. The solid line (colored red in the online version) represents the fiducial ridgeline. (b) Same as (a) but for cluster L6. (c) Same as (a) but for cluster L110.

(A color version of this figure is available in the online journal.)

reddening (Piatti et al. 2005), and indeed lie very close together in the outer parts of the SMC, but L4 is more metal-rich than L6. Therefore, the L4 fiducial should be redder than that of L6. For this reason, we had to adopt $E(B-V)$ values larger than the ones reported in the literature (0.03 and 0.04 for L4 and L6, respectively; Piatti et al. 2005). This problem is likely due to the fact that L4 and L6 were observed on the same CTIO 1 m frame, which was centered on L6, leaving L4 located near the image border. It is well known that objects observed in the border of such images may have a difference of up 0.05 mag with respect to the centered objects.

From this procedure we find than the two clusters have ages of ∼7 Gyr. While our photometric calibration is not precise enough to consider these ages robustly determined, it is important to note that they constitute an independent confirmation of the truly old nature of these clusters.

6. AGE ANALYSIS

In the previous section, it was demonstrated that the combination of the δV parameter and CC94 calibration is a very good indicator of cluster age. For the subsequent analysis, we then adopted values of cluster ages derived in the present work

11
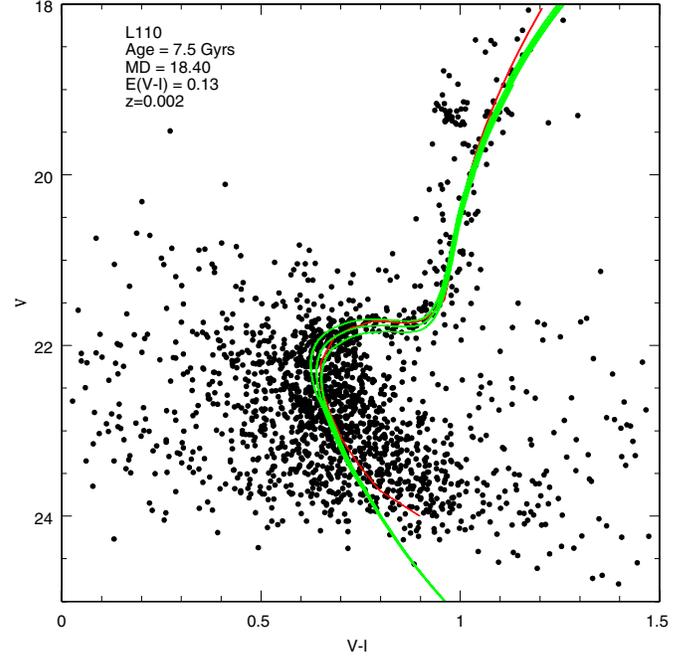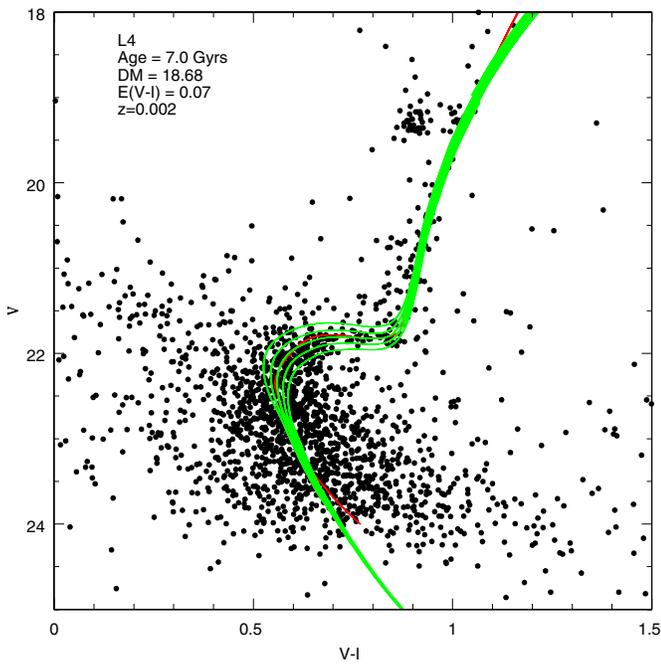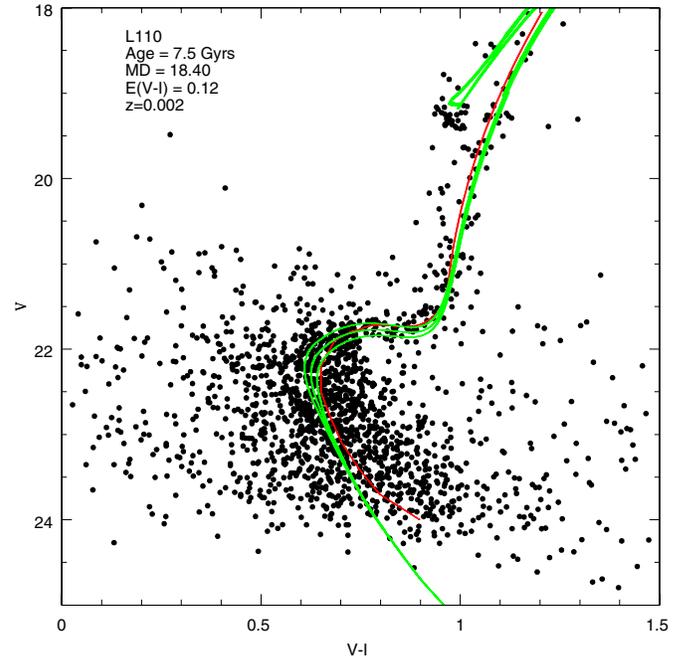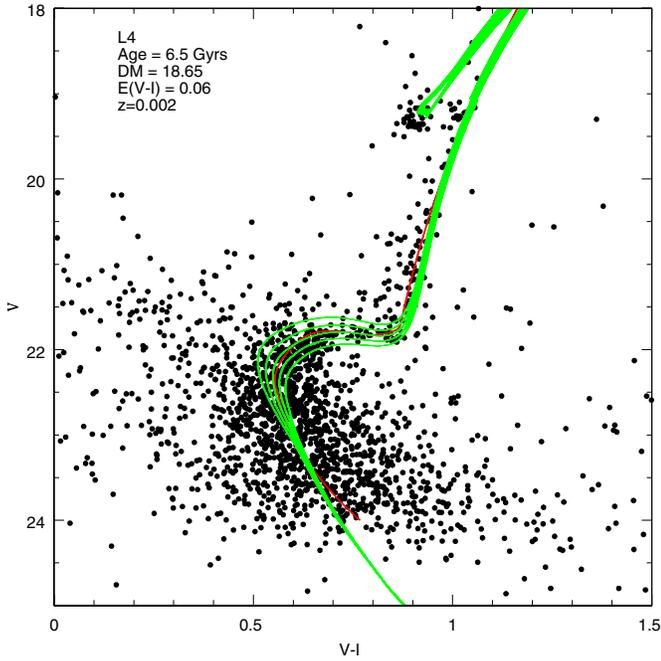
Figure 8. CMD of L4. Upper panel: we show Teramo isochrones as solid lines (colored green in the online version). They cover an age range of 5.5–7.7 Gyr in steps of 0.5 Gyr. The central isochrone ($z = 0.002$), which best reproduces the fiducial ridgeline (red line in the online version), is the one that we have adopted. Fitting parameters are listed in the plot. Lower panel: same as the upper panel but for Dartmouth isochrones in age steps of 6, 6.5, 7, 7.5, and 8 Gyr.

(A color version of this figure is available in the online journal.)

Figure 9. CMD of L110. Upper panel: we show Teramo isochrones as solid lines (colored green in the online version). They cover an age range of 7–8 Gyr in steps of 0.5 Gyr. The central isochrone ($z = 0.002$), which best reproduces the fiducial ridgeline (red line in the online version), is the one that we have adopted. Fitting parameters are listed in the plot. Lower panel: same as the upper panel but for Dartmouth isochrones in age steps of 7, 7.5, and 8 Gyr.

(A color version of this figure is available in the online journal.)

using the CC94 calibration and metallicities from Paper I. As a consequence, the ages and metallicities of our sample of 15 SMC clusters were determined homogeneously and on the same scale. We believe our errors in both age and metallicity to be significantly smaller than in other works (e.g., Piatti 2011a, 2011b; Piatti et al. 2011), as well as being homogeneously derived. However, even though our sample is homogeneous, it is limited to only 15 clusters. In order to study global effects, a larger sam-

ple is necessary. We now proceed to enlarge the cluster sample as carefully as possible.

6.1. Age Distribution

The age distribution (AD) of a sample of star clusters is a very valuable tool that allows us to understand cluster formation processes. Until about a decade ago, it was widely believed that the SMC formed its clusters continuously over the last 12 Gyr (Olszewski et al. 1996; van den Bergh 1991; Da Costa & Hatzidimitriou 1998, hereafter DH98), while the AD of star

Figure 11. SMC age distribution. Lined histogram: 15 clusters from this work. Empty histogram: 5 clusters from Piatti et al. (2001), 2 from Piatti et al. (2007b), 9 from Piatti (2011a), 7 from Piatti et al. (2011), 11 from Piatti (2011b), ESO 51-SC09 (this work and Piatti 2012), and 15 from this work.

Figure 10. CMD of L6. Upper panel: we show Teramo isochrones as solid lines (colored green in the online version). They cover an age range of 6–8 Gyr in steps of 0.5 Gyr. The central isochrone ($z = 0.001$), which best reproduces the fiducial ridgeline (red line in the online version), is the one that we have adopted. Fitting parameters are listed in the plot. Lower panel: same as the upper panel but for Padova isochrones in age steps of 6.3, 7.08, and 7.94 Gyr.

(A color version of this figure is available in the online journal.)

clusters in the LMC was known to have the infamous age gap (Da Costa 1991). Rich et al. (2000) presented the first compelling evidence for bursts in cluster formation in SMC clusters. They reported *HST* photometry and MSTO ages for seven SMC clusters older than 1 Gyr and they analyzed the AD of their cluster sample together with the sample previously studied by DH98. They found two peaks in the AD at 2 ± 0.5 and 8 ± 2 Gyr. More recently, however, Glatt et al. (2008b), using superior *HST* photometry for seven clusters, found no evidence of two cluster

formation bursts, although their AD reveals a slight enrichment in the cluster formation process at 6 Gyr. Although the Glatt et al. (2008b) ages were accurately determined, their sample is statistically very small. On the other hand, Piatti et al. (2011) obtained the most complete SMC AD using 43 star clusters with age estimates (see their Table 19) derived in their paper and supplemented by ages taken from the literature. The AD derived by these authors presents bimodality, showing two peaks of enhanced star formation processes at $t \sim 2$ and 5 Gyr. Their AD also shows that the slope in the cluster formation/destruction rate is constant from 12 to ~ 8 Gyr. According to these authors, this may reflect the possibility that in this period there existed a constant cluster formation rate, in agreement with the simple closed box model presented by DH98.

The crosshatched histogram in Figure 11 shows the AD obtained for the present 15 cluster sample. Unfortunately, our sample is too small to draw definitive conclusions. For this reason, we decided to add other previously studied clusters to our sample, trying to maintain age homogeneity as far as possible. Piatti et al. systematically studied SMC star clusters from Washington photometry. In a series of papers they calculated the δT_1 parameter as the difference between the T_1 magnitude of the RC and the MSTO. We selected 27 clusters from Piatti et al. (2001, 2007b) and Piatti (2011a, 2011b). We transformed their δT_1 values into δV by inverting Equation (3) of Geisler et al. (1997). We also included the age value of ESO 51-SC09 (5.2 ± 0.4 Gyr) derived in Section 5 using the CC94 calibration. Next, we calculated cluster ages using the CC94 calibration to place Piatti et al.'s cluster ages on the same scale as ours. Piatti et al. (2011) derived the ages of 14 SMC clusters (8 of them not included in our sample) from the δT_1 parameter. These authors did not include the δT_1 values but we estimated them from the published CMDs. We did not include the cluster IC 1708 because its CMD does not have an evident clump. In Table 3, we list cluster designation, δT_1 with its error, the reference from

Table 3
Washington Cluster Sample

Cluster	δT_1	Ref.	δV	t_C
K28	1.70 ± 0.30	1	1.57 ± 0.30	2.0 ± 0.3
K44	2.10 ± 0.20	1	1.97 ± 0.20	3.0 ± 0.3
L116	2.00 ± 0.40	1	1.87 ± 0.40	2.7 ± 0.5
L32	2.50 ± 0.10	1	2.37 ± 0.10	4.6 ± 0.2
L38	2.70 ± 0.10	1	2.58 ± 0.10	5.6 ± 0.3
L112	2.60 ± 0.15	2	2.47 ± 0.15	5.1 ± 0.3
L113	2.35 ± 0.15	2	2.22 ± 0.15	3.9 ± 0.3
AM 3	2.70 ± 0.15	3	2.58 ± 0.15	5.6 ± 0.4
HW 31	2.50 ± 0.15	3	2.37 ± 0.15	4.6 ± 0.3
HW 40	2.60 ± 0.15	3	2.47 ± 0.15	5.1 ± 0.3
HW 41	2.70 ± 0.15	3	2.58 ± 0.15	5.6 ± 0.4
HW 42	3.10 ± 0.15	3	2.98 ± 0.15	8.5 ± 0.6
HW 59	2.80 ± 0.15	3	2.68 ± 0.15	6.2 ± 0.4
HW 63	2.60 ± 0.15	3	2.47 ± 0.15	5.1 ± 0.3
L91	2.40 ± 0.15	3	2.27 ± 0.15	4.1 ± 0.3
NGC 339	2.60 ± 0.15	3	2.47 ± 0.15	5.1 ± 0.3
L3	0.80 ± 0.25	4	0.66 ± 0.25	0.8 ± 0.1
L28	0.75 ± 0.25	4	0.61 ± 0.25	0.7 ± 0.1
HW 66	2.20 ± 0.25	4	2.08 ± 0.25	3.4 ± 0.4
L100	1.80 ± 0.25	4	1.67 ± 0.25	2.2 ± 0.3
HW 79	2.40 ± 0.25	4	2.27 ± 0.25	4.1 ± 0.5
L109	2.20 ± 0.25	4	2.07 ± 0.25	3.3 ± 0.4
HW 85	1.75 ± 0.25	4	1.62 ± 0.25	2.1 ± 0.2
B34	1.20 ± 0.15	5	1.06 ± 0.15	1.2 ± 0.1
B39	1.20 ± 0.20	5	1.06 ± 0.20	1.2 ± 0.1
B47	1.10 ± 0.30	5	0.96 ± 0.30	1.1 ± 0.1
B112	1.30 ± 0.15	5	1.16 ± 0.15	1.3 ± 0.1
BS 88	1.60 ± 0.15	5	1.46 ± 0.15	1.8 ± 0.1
HW 22	2.70 ± 0.20	5	2.58 ± 0.20	5.6 ± 0.5
HW 55	1.90 ± 0.30	5	1.77 ± 0.30	2.4 ± 0.3
HW 67	2.00 ± 0.20	5	1.87 ± 0.20	2.7 ± 0.3
K38	2.10 ± 0.35	5	1.97 ± 0.35	3.0 ± 0.4
L58	1.60 ± 0.20	5	1.46 ± 0.20	1.8 ± 0.2
NGC 419	1.10 ± 0.25	5	0.96 ± 0.25	1.1 ± 0.1

References. (1) Piatti et al. 2001; (2) Piatti et al. 2007b; (3) Piatti 2011a; (4) Piatti et al. 2011; (5) Piatti 2011b.

which δT_1 was taken, δV, and the corresponding ages with their respective errors.

Therefore, our full sample now consists of a total of 50 clusters with ages on the same scale, comparable to the sample used by Piatti et al. (2011). In relation to the Piatti et al. (2011) work, it is worth pointing out that they use an age scale where L1 is 10 Gyr (Mighell et al. 1998), although the best age determination for L1 is 7.5 Gyr (Glatt et al. 2008b). Similarly, Piatti gives an age for NGC 121 of 12 Gyr and K3 of 9 Gyr, while the corresponding Glatt et al. values are 10.5 and 6.5, respectively. Thus, it appears that the Piatti et al. scale is indeed somewhat different from the one adopted here, especially for the oldest clusters.

The unhatched histogram of Figure 11 represents the AD of the extended sample. Figure 11 reproduces the two peaks found in Piatti et al. (2011) at ∼2 and ∼5 Gyr. They suggest that the two peaks correspond to bursting cluster formation episodes. Very recently, Weisz et al. (2013) derived large scale field star formation histories of both Clouds from deep *HST* imaging of a number of regions. They find two notable peaks in the SMC, at ∼4.5 and ∼9 Gyr ago, which are not present in the LMC. They also find sharp increases in the star formation history of both galaxies starting about 3.5 Gyr ago. One of course expects that the field and cluster formation histories should be very similar.

We do find a good correspondence with the strong increase starting 3.5 Gyr ago, and reasonable agreement with the peak about 4.5–5 Gyr ago. The field stars also appear to show a peak around 2 Gyr ago, as we find in the clusters. However, the cluster sample is too small to discern any structure earlier than 6.5 Gyr ago, in particular to corroborate or not the field star peak at 9 Gyr.

Our sample does not appear to show a constant slope for the first ∼4 Gyr of the SMC, as posed by Piatti et al. (2011). In any case, the numbers are very small and the statistics are therefore very uncertain. Note that the ages of L4 and L6 included in the sample of Piatti et al. (2011) are the ones derived by Piatti et al. (2005), which have been considerably underestimated, as we have shown in Section 4. Consequently, the conclusions reached by Piatti et al. (2011) could substantially change if these authors used our ages for L4 and L6, which should be much more accurate. Similarly, some of the cluster ages included in our extended sample could also have been underestimated because the clusters were observed with small telescopes (especially those in Piatti et al. 2001 and Piatti et al. 2007b). In these cases, the real MSTO T_1 magnitude may not have been clearly detected. Although our sample of 15 star clusters is not large enough to either confirm or deny the existence of the first burst of star formation at 5 Gyr and/or the constant slope for the first ∼4 Gyr, the photometry of our 15 clusters is deep enough to measure the MSTO with small errors. This fact, together with the homogeneous nature of our 15 cluster ages, supports the existence of the second peak of star formation at 2 Gyr suggested by Piatti et al. (2011, crosshatched AD). It is clearly advisable to continue studying clusters in a homogeneous way, applying the same techniques. With this in mind, we have obtained *V* and *I* images and spectra in the CaT region of an additional sample of 15 clusters. Currently, we are in the process of deriving ages and metallicities following the same procedures used here and in Paper I. We are confident that such a homogeneous sample of 30 clusters will enable us to better understand the processes of cluster formation in the SMC.

6.2. Age Gradient

To take into account the orientation of the SMC and the probable projection effects necessary to analyze the possible existence of an SMC gradient, we adopted the elliptic system defined in Piatti et al. (2007a). In this system, the semimajor axis *a* is used instead of the true cluster galactocentric distance (see Piatti et al. 2007a and P09 for details on the calculation of *a*).

In Figure 12 we show how cluster ages vary as a function of *a*. Filled circles represent our 15 clusters, which show no evidence of an age gradient. We also included in Figure 12 the additional 35 clusters studied by Piatti et al. (see the above description and figure caption for details). The extended sample also supports the nonexistence of an age gradient as has been previously suggested by other authors (see, e.g., Piatti 2011b; Glatt et al. 2008b). Note that in Paper I we find no metallicity gradient either. It is necessary to note, however, that the spatial distributions of age and metallicity are built based on the current positions of the clusters. To find out where they were born it would be necessary to know their orbits, which at present is not possible.

The Weisz et al. (2013) study of the large scale field star formation history of the Clouds finds that after the onset of the recent strong increase in star formation some 3.5 Gyr ago in the SMC, subsequent star formation was concentrated in the
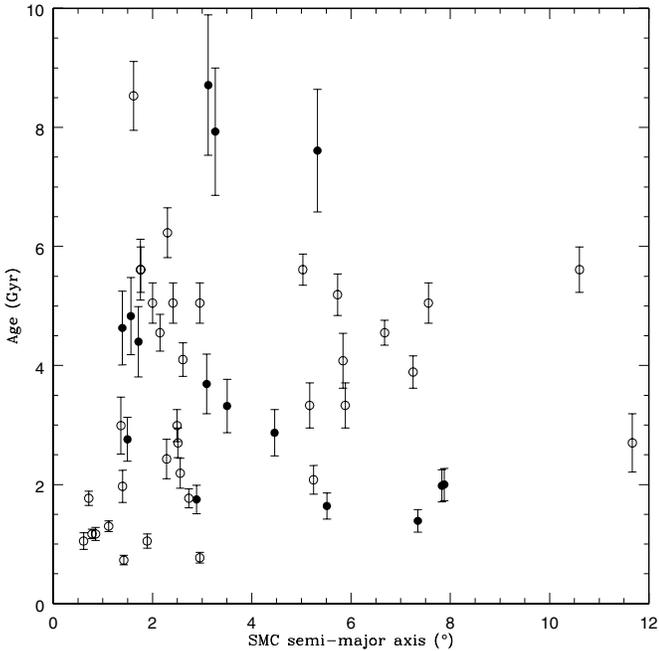
Figure 12. Age vs. semimajor axis *a* for 15 clusters from this work plotted as filled circles, and 5 from Piatti et al. (2001), 2 from Piatti et al. (2007b), 9 from Piatti (2011a), 7 from Piatti et al. (2011), 11 from Piatti (2011b), and ESO 51-SC09 (this work and Piatti 2012) plotted as open circles.

central regions of the galaxy and little or no field star formation occurred outside this area. Their sampling is small, however, as they only have fields at a galactocentric radius of about 0.5 kpc or 2.3 kpc, which correspond to ∼1 and 4°.6. However, we clearly have a number of young clusters located beyond this radius in our diagram. Either the Weisz et al. sample is too small and does not reveal real variations in the galaxy, or the field and cluster star formation is uncoupled, which is less likely. We believe that the clusters are telling us more of the true star formation history and that recent star formation is not solely concentrated in the central regions.

7. AGE–METALLICITY RELATION

The relationship between the age of a stellar population and the overall metallicity and its time variation, is one of the best tools to study the chemical evolutionary history of a galaxy. Both the ages and metallicities of the tracer population need to be as accurately determined as possible. It is of vital importance for those parameters not only to be on the same scale but also to be determined in a homogeneous way.

Several investigations have aimed to derive the SMC AMR using various stellar populations, such as star clusters, field giants, and planetary nebulae (see, e.g., Stryker et al. 1985; Da Costa 1991; Olszewski et al. 1996).

After these first attempts, DH98 obtained what can be considered the first well-constrained SMC AMR. DH98 used a sample of six clusters studied by them and others. Their metallicities were determined from CaT spectra and their ages from deep, ground-based CMDs. According to DH98, the metallicity variation with age in the SMC is consistent with a simple closed box model. However, subsequent analyses seemed to be more in agreement with only a small increase in the intermediate period followed more recently by a faster evolution.

A series of papers summarized in Piatti et al. (2007c), wherein cluster ages and abundances were derived from Washington photometry, showed an excellent agreement with the bursting model of Pagel & Tautvaišienė (1998, hereafter PT98), even in the intermediate period ranging from 5 to 10 Gyr. The PT98 model assumes an early burst, followed by no star formation from ∼12–4 Gyr ago, and then an ensuing burst of recent star formation, leading to a significantly enhanced subsequent enrichment. However, in Paper I, we showed that there is poor agreement between our CaT observations and the PT98 model for the intermediate period.

The recent investigation of Piatti (2011a) confirms our point of view that, although the PT98 model is a very good representation of the observations for ages smaller than 4 Gyr, this model fails to explain the AMR for larger ages. In fact, the nine SMC clusters studied by Piatti (2011a) are older than 4 Gyr but cover a considerable metallicity range. More precisely, eight of their nine clusters are included within a very small age range ($\Delta t = 2.2$ Gyr) but their metallicities vary from -0.7 to -1.3 dex, five of which have metallicity values considerably larger than those predicted by PT98.

In Paper I we also found that some of our clusters have metallicities in good agreement with the models of Carrera (2005) and Carrera et al. (2008), which do not assume any bursts but use instead both infall and outflow. Carrera et al. used the CaT to derive metallicities on the Carretta & Gratton (1997) scale for a large number of field giants in regions spread across the SMC. In Paper I we concluded that the model of PT98 is a good representation of the AMR for ages < 3–4 Gyr but the ideal model for larger ages would predict metallicities between PT98 and the Carrera (2005) and Carrera et al. (2008) models.

As we have already mentioned, in Paper I we analyzed the AMR of the SMC using our sample of 15 SMC clusters as tracers. The metallicities of these clusters were accurately determined following the CaT technique so that they are on a homogeneous scale. Unfortunately, at the time of Paper I, we could not determine ages for these objects from our own data, instead simply taking them from the literature. So the AMR of Paper I is inhomogeneous regarding ages. The CaT method is among the most accurate procedures for the determination of cluster metallicities (Cole et al. 2004; Grocholski et al. 2006) and the δV parameter is an excellent age indicator (e.g., Carraro & Chiosi 1994), so the AMR derived in the current work can be considered a good indicator of the chemical evolution of the SMC and a significant improvement over Paper I given the now homogeneous ages.

In Figure 13 we present our new AMR. Solid circles represent our 15 cluster sample considering ages derived in this work and metallicities from Paper I.

As in Paper I, we have also included in Figure 13 six clusters with metallicities derived by other authors on the same scale as ours, namely three from DH98 (open circles) and another three from Glatt et al. (2008b), with their metallicities derived by the CaT method. We only included clusters that we do not have in common with other studies, using in these cases the metallicity values on the Carretta & Gratton (1997) scale to match ours. We have also included NGC 330, whose metallicity (-0.94 ± 0.2) was derived by Gonzalez & Wallerstein (1999) from high resolution spectroscopy. Squares in Figure 13 represent the mean CaT metallicities calculated by Carrera et al. (2008) in different age bins for their sample of field stars. Different lines represent (1) the model of closed box continuous star formation computed by DH98 (short-dashed line), (2) the bursting model
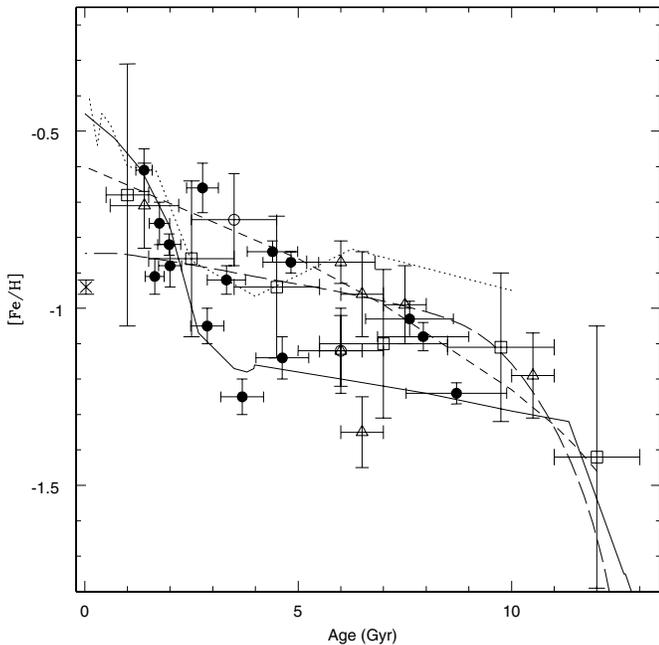
Figure 13. Filled circles stand for clusters of our sample. The cross marks cluster NGC 330 (Gonzalez & Wallerstein 1999). Squares show the mean metallicities in six age bins calculated by Carrera et al. (2008). The short-dashed line represents the model of closed box continuous star formation computed by Da Costa & Hatzidimitriou (1998). The long-dashed line shows the best-fit model derived by Carrera (2005). The solid line represents the bursting model of Pagel & Tautvaišienė (1998). Finally, the dotted line stands for the AMR obtained by Harris & Zaritsky (2004).

gap really is. Accurate ages and metallicities for more clusters, on a homogeneous scale, are also of paramount importance to derive a definitive understanding of the chemical evolution of this important galaxy.

8. SUMMARY AND CONCLUSIONS

We measured the parameter δV in the V versus $V - I$ CMDs of 15 SMC star clusters and we used the calibrations of CC94 to derive their ages. We found that three of them, L110, L4, and L6, are newly discovered very old SMC clusters ($t = 7.6 \pm 1.0$, 7.9 ± 1.1, and 8.7 ± 1.2, respectively). Consequently, we have considerably enlarged the number of known old clusters in this galaxy. We corroborate the old nature of these new old clusters from two independent methods. First, we derived a new calibration (SMC δ calibration) using the SMC clusters studied by Glatt et al. (2008a, 2008b) with deep *HST* photometry. Second, we calibrated our VLT photometry with independent observations and we fitted different sets of isochrones to the calibrated CMDs of these old clusters.

Finally, using ages derived from the combination of δV and CC94's calibration, and metallicities from Parisi et al. (2009), we analyzed the AD, age gradient, and the AMR of the SMC. Our main results are as follows.

1. We combined our 15 SMC clusters with 35 clusters studied by other authors. The AD of this combined sample of 50 clusters reproduces the two peaks found in Piatti et al. (2011) at ~ 2 and ~ 5 Gyr (corresponding to possible episodes of cluster formation), but it does not show a constant slope in the AD for the first ~ 4 Gyr. The peak at 5 Gyr is in reasonable agreement with the peak in the field star formation rate at about 4.5 Gyr found recently by the *HST* study of Weisz et al. (2013), but their second peak at 9 Gyr is not found in our data.

2. The extended sample supports the idea of the nonexistence of an age gradient, as has been previously suggested by other authors (see, e.g., Piatti 2011b; Glatt et al. 2008b). In particular, we find clusters younger than 3.5 Gyr at a large range of galactocentric distances and not just near the center, as suggested by the field star data of Weisz et al. (2013).

3. Combining our cluster sample with those observed by DH98 and Glatt et al. (also with CaT) and the one cluster with high resolution metallicity, we compiled a sample of 25 clusters on a homogeneous metallicity scale with relatively small errors and studied the cluster AMR. We corroborate our Paper I result that for ages smaller than ~ 4 Gyr, the chemical enrichment of the SMC is well represented by the PT98 model, but for explaining the intermediate/old SMC period a more complicated model is needed. We now have seven clusters older than 6 Gyr homogeneously studied so we have doubled the representation of that period.

4. According to the calibration of CC94, our three new old clusters lie between L1 and NGC 121, which suggests that the suggested SMC cluster age gap claimed by Glatt et al. (2008a) is probably not real.

of PT98 (solid line), (3) the best-fit model derived by Carrera (2005, long-dashed line), and (4) the AMR obtained by Harris & Zaritsky (2004).

If we first consider only our 15 cluster sample, the main differences that we can find between the present AMR and the one derived in Paper I, are: (1) The ages of clusters younger than 4 Gyr are now in better agreement with the model of PT98; (2) We now have six star clusters with ages larger than 4 Gyr so we have improved the representation of the intermediate/old SMC period. Four of these six clusters follow reasonably well both the DH98 and Carrera (2005) models, but the other two intermediate/old clusters are better represented by the model of PT98; (3) We have found three new very old SMC clusters and two of them, L4 and L6, are right next to each other in the very outer reaches of the SMC; and (4) These three old clusters are candidates for filling the possible "SMC age gap." Their newly determined accurate ages and abundances allow improved understanding of the AMR for the old period, particularly between L1 and NGC 121.

Considering the full cluster sample, we corroborate that the model of PT98 is a good indicator of the chemical enrichment of the SMC for ages less that 4 Gyr (except for the anomalous cluster NGC 330), but a more complicated model is needed to account for the intermediate/old SMC period. The PT98 model underestimates metallicities during this period. It is clear that the chemical evolution was slow during this period and then experienced an increase during the last few Gyr, as discussed extensively in Paper I. However, the sample size is still small, especially for older clusters. Continued searches for such undiscovered old clusters will be important to try and pin down the chemical evolution and cluster formation history during this time, and to see how real the possible SMC age

Facility: VLT:Antu (FORS2)

REFERENCES

Anthony-Twarog, B. J., & Twarog, B. A. 1985, ApJ, 291, 595
Beasley, M., Hoyle, F., & Sharples, R. M. 2002, MNRAS, 336, 168
Bertelli, G., Bressan, A., Chiosi, C., Fagotto, F., & Nasi, E. 1994, A&AS, 106, 275
Cannon, R. D. 1970, MNRAS, 150, 111
Carraro, G., & Chiosi, C. 1994, A&A, 287, 761 (CC94)
Carrera, R. 2005, PhD thesis, Departamento de Astrofísica, Universidad de La Laguna, España
Carrera, R., Gallart, C., Aparicio, A., et al. 2008, AJ, 136, 1039
Carretta, E., & Gratton, R. G. 1997, A&AS, 121, 95
Cole, A. A., Smecker-Hane, T. A., Tolstoy, E., Bosler, T. L., & Gallagher, J. S. 2004, MNRAS, 347, 367
Crowl, H. H., Sarajedinini, A., Piatti, A. E., et al. 2001, AJ, 122, 220
Da Costa, G. S. 1991, in IAU Symp. 148, The Magellanic Clouds, ed. R. Haynes & D. Milne (Dordrecht: Kluwer), 183
Da Costa, G. S., & Hatzidimitriou, D. 1998, AJ, 115, 1934 (DH98)
Dotter, A., Chaboyer, B., Jevremović, D., et al. 2007, AJ, 134, 376
Dotter, A., Sarajedini, A., Anderson, J., et al. 2010, ApJ, 708, 698
Dutra, C. M., Bica, E., Clariá, J. J., & Piatti, A. E. 1999, MNRAS, 305, 373
Ferraro, F. R., Fusi Pecci, F., Testa, V., et al. 1995, MNRAS, 272, 391
Geisler, D., Bica, E., Dottori, H., et al. 1997, AJ, 114, 1920
Girardi, L., Bressan, A., Bertelli, G., & Chiosi, C. 2000, A&AS, 141, 371
Girardi, L., Dalcanton, J., Williams, B., et al. 2008, PASP, 120, 583
Glatt, K., Gallagher, J. S., III, Grebel, E. K., et al. 2008a, AJ, 135, 1106
Glatt, K., Grebel, E. K., Sabbi, E., et al. 2008b, AJ, 136, 1703
Gonzalez, G., & Wallerstein, G. 1999, AJ, 117, 2286
Grocholski, A. J., Cole, A. A., Sarajedini, A., Geisler, D., & Smith, V. 2006, AJ, 132, 1630
Harris, J., & Zaritsky, D. 2004, AJ, 127, 1531
Janes, K. A., & Phelps, R. L. 1994, AJ, 108, 1773 (JP94)
Landolt, A. 1992, AJ, 104, 340
Marigo, P., Girardi, L., Bressan, A., et al. 2008, A&A, 482, 883
Mighell, K. J., Sarajedini, A., & French, R. S. 1998, AJ, 116, 2395
Olszewski, E. W., Suntzeff, N. B., & Mateo, M. 1996, ARA&A, 34, 511
Pagel, B. E. J., & Tautvaišienė, G. 1998, MNRAS, 299, 535 (PT98)
Parisi, M. C., Grocholski, A. J., Geisler, D., Sarajedini, A., & Clariá, J. J. 2009, AJ, 138, 517 (Paper I)
Phelps, R. L., Janes, K. A., & Montgomery, K. A. 1994, AJ, 107, 1079
Piatti, A. E. 2011a, MNRAS, 416, L89
Piatti, A. E. 2011b, MNRAS, 418, L69
Piatti, A. E. 2012, ApJL, 756, L32
Piatti, A. E., Clariá, J. J., Bica, E., et al. 2011, MNRAS, 417, 1559
Piatti, A. E., Santos, J. F. C., Clariá, J. J., et al. 2001, MNRAS, 325, 792
Piatti, A. E., Sarajedini, A., Geisler, D., Clark, D., & Seguel, J. 2007a, MNRAS, 377, 300
Piatti, A. E., Sarajedini, A., Geisler, D., Gallart, C., & Wischnjewsky, M. 2007b, MNRAS, 381, L84
Piatti, A. E., Sarajedini, A., Geisler, D., Gallart, C., & Wischnjewsky, M. 2007c, MNRAS, 382, 1203
Piatti, A. E., Sarajedini, A., Geisler, D., Seguel, J., & Clark, D. 2005, MNRAS, 358, 1215
Pietrinferni, A., Cassisi, S., Salaris, M., & Castelli, F. 2004, ApJ, 612, 168
Rafelski, M., & Zaritsky, D. 2005, AJ, 129, 2701
Rich, R. M., Shara, M., Fall, S. M., & Zurek, D. 2000, AJ, 119, 197
Rosenberg, A., Saviane, I., Piotto, G., & Aparicio, A. 1999, AJ, 118, 2306
Salaris, M., & Weiss, A. 1997, A&A, 327, 107
Salaris, M., Weiss, A., & Percival, M. 2004, A&A, 414, 163 (S04)
Sarajedini, A., & Demarque, P. 1990, ApJ, 365, 219
Stetson, P. B. 1987, PASP, 99, 191
Storm, J., Carney, B. W., Gieren, W. P., et al. 2004, A&A, 415, 531
Stryker, L. L., Da Costa, G. S., & Mould, J. R. 1985, ApJ, 298, 544
Vandenberg, D. A., Bolte, M., & Stetson, P. B. 1990, AJ, 100, 445
van den Bergh, S. 1991, ApJ, 369, 1
Weisz, D. R., Dolphin, A. E., Skillman, E. D., et al. 2013, MNRAS, 431, 364